Environmental Pollution 344 (2024) 123406

Contents lists available at ScienceDirect

Environmental Pollution

journal homepage: www.elsevier.com/locate/envpol

Effects of extreme precipitation on bacterial communities and bioaerosol composition: Dispersion in urban outdoor environments and health risks☆

Ting Zhang [a], Dingqiang Zhang [a], Zhonghang Lyu [a], Jitao Zhang [a], Xian Wu [a], Yingxin Yu [b,c,*]

[a] College of Civil Engineering, Liaoning Technical University, Fuxin, 123000, China
[b] Guangdong-Hong Kong-Macao Joint Laboratory for Contaminants Exposure and Health, Guangdong Key Laboratory of Environmental Catalysis and Health Risk Control, Institute of Environmental Health and Pollution Control, Guangdong University of Technology, Guangzhou, 510006, China
[c] Guangzhou Key Laboratory of Environmental Catalysis and Pollution Control, Key Laboratory of City Cluster Environmental Safety and Green Development of the Ministry of Education, School of Environmental Science and Engineering, Guangdong University of Technology, Guangzhou, 510006, China

ARTICLE INFO

Handling Editor: Admir Créso Targino

Keywords:
Seasonal precipitation
Bioaerosol
Bacterial community
Health risk
Air quality

ABSTRACT

Concerns about contaminants dispersed by seasonal precipitation have grown due to their potential hazards to outdoor environments and human health. However, studies on the crucial environmental factors influencing dispersion changes in bacterial communities are limited. This research adopted four-season in situ monitoring and sequencing techniques to examine the regional distribution profiles of bioaerosols, bacterial communities, and risks associated with extreme snowfall versus rainfall events in two monsoon cities. In the early-hours of winter snowfall, airborne cultivable bioaerosol concentrations were 4.1 times higher than the reference exposure limit (500 CFU/m^3). The concentration of ambient particles (2.5 μm) exceeded 24,910 particles/L (97 μg/m^3), positively correlating with the prevalence of cultivable bioaerosols. These bioaerosols contained cultivable bacterial species such as pathogenic *Staphylococcus aureus*, *Staphylococcus epidermidis*, *Streptococcus pneumoniae*, and *Escherichia coli*. Bioaerosol concentrations increased by 53.0% during 50-mm snow extremes. Taxonomic analysis revealed that Pseudomonas, Staphylococcus, and Veillonella were the most abundant bacterial taxa in the initial snowmelt samples during winter precipitation. However, their abundance decreased by 87.6% as snowing continued (24 h). Reduced water base cation concentration also led to a 1.15-fold increase in the Shannon index, indicating a similar yet heightened bacterial diversity. Seasonally, Pedobacter and Massilia showed higher relative abundance (25% and 18%, respectively), presenting increased bacterial transmission to the soil. Furthermore, Pseudomonas was identified in 60% of spring snowstorm samples, suggesting long-distance dispersal of pathogenic bacteria. When these atmospheric aerosol particles carrying biological entities (0.65–1.1 μm) penetrated human alveoli, the calculated hazard ratio was 0.55, which as observed in inhalation exposures. Consequently, this study underscores the risk of seasonal precipitation-enhanced ambient bacterial transmission.

1. Introduction

Climate warming is increasing extreme precipitation events, making them more likely to occur in highly urbanized areas (Lei et al., 2023; Hemmati et al., 2022; Zhang et al., 2020a). Biological ice nucleation, such as *Lysinibacillus* genus, contributes to a growing body of precipitation evidence, dominating atmospheric bacterial deposition and resulting in differences in bacterial communities (Failor et al., 2017; Huang et al., 2021, Woo and Yamamoto, 2020). Microbial ice nucleation can amplify the biological concentrations in seasonal precipitation (such as bacteria associated with rain, sleet, and snow), leading to the descent of inhalable bacterial pathogens (Failor et al., 2017). While the dispersion of snow and rain precipitation into urban outdoor environments is considered normal, its effects on air, water, and soil pollution, changes in microbial community distribution, and potential risks remain contentious.

Outdoor workers are susceptible to bacteria during intense snowfalls or rainfalls (Chemke et al., 2022; Hu et al., 2019; Wei et al., 2020).

☆ This paper has been recommended for acceptance by Admir Créso Targino.

* Corresponding author. Guangdong-Hong Kong-Macao Joint Laboratory for Contaminants Exposure and Health, Guangdong Key Laboratory of Environmental Catalysis and Health Risk Control, Institute of Environmental Health and Pollution Control, Guangdong University of Technology, Guangzhou, 510006, China.
E-mail address: yuyingxin@gdut.edu.cn (Y. Yu).

https://doi.org/10.1016/j.envpol.2024.123406
Received 22 August 2023; Received in revised form 17 January 2024; Accepted 18 January 2024
Available online 18 January 2024

Various bacteria from the phylum Firmicutes (Antony et al., 2016; Liu et al., 2006) have been detected in snow, potentially leading to unforeseen infectious diseases (Uk Lee et al., 2016). These microbiomes in snow and rain comprise representatives from 25 distinct phyla, surpassing historically recorded maximums (Behrangi et al., 2016; Jeznach et al., 2017; Routson et al., 2019). The recent "bio-precipitation" with "rain-making" bacteria transmission might be more hazardous than previously assumed (Monteil et al., 2014; Schiermeier, 2008). Exacerbated by anthropogenic emissions and urbanization influences, the atmospheric dispersion of microbial entities during extreme precipitation can severely impact climate model uncertainties, and poor observation characteristics (Madakumbura et al., 2021). More recent studies have detected human-related particulate matter and microbial emissions discharged into the urban surface from urbanization and industrialization, which are transported along the water cycle (Mardonova and Han, 2023; Lou et al., 2021). However, precipitation-related biological risks remain underexplored, partly due to some misconceptions about the contributions of biological species (Cariñanos et al., 2021).

The relatively low diversity and medium complexity of microbial assemblages enables them to survive or even thrive in extreme snowpack environments (Van Leuken et al., 2016). Reports have noted significant fluctuations in the diversity of microbial communities during heavy rainfall events (Šťovíček et al., 2017). Quantifying the variations in unexpectedly dominant species during increased extreme precipitation events is crucial, though challenging (Georgescu et al., 2021). A modelling approach for certain snow-origin bacteria can delineate their dominance throughout the hydrologic cycle (Liu et al., 2021). Spearman's rank correlation analysis has confirmed a positive causal link between the abundance of Firmicutes and soil pollution (Zhang et al., 2020b). On-site sampling and in-situ experiments have identified cultivable bacteria, such as Pseudomonas (including *Pseudomonas aeruginosa*). These pathogenic bacteria that can infect humans (Dean and Mitchell, 2020).

In recent years, 16 S rDNA gene sequencing-based microbial profiling has become vital for quantitative analysis (Park et al., 2021). To gather reliable bioaerosol data, some annual studies (O'Connor et al., 2015) recommended to use an in-situ, size-selective Andersen sampler to collect airborne cultivable bioaerosols (Haas et al., 2020). Quantitative polymerase chain reaction (qPCR) ascertains the microbial composition of environmental samples, while an amplicon sequencing approach can determine the levels of bacterial species (Dreier et al., 2022). These findings underscore scientists' viewpoint that considering bioaerosols' genomic properties is a promising method for investigating the transmission of environmental microbes in urban areas (Peiffer et al., 2021; Zimmerman et al., 2020).

Atmospheric factors influence variations in urban bacterial communities across various geographical regions (Ruiz-Gil et al., 2020). The airborne abundance, community patterns, and microbial size distribution differ between non-hazy and hazy conditions (Hu et al., 2020). In the southeastern United States, a stronger source of ice-nucleating coarse bioaerosols was observed compared to long-range transported dust or summertime marine emissions in Mexico (Ziemba et al., 2016). Also, misty conditions can facilitate microbial transport due to light droplet-induced aerosol generation, thereby increasing disease spread (Joung et al., 2017). Increased rainfall or snowfall can result in a "washout" effect, lowering airborne particle concentrations. However, studies on the crucial environmental factors affecting changes in dispersed bioaerosol communities are limited (Schramm et al., 2021).

Pathogenic bioaerosol-bound components have been detected in the human respiratory systems (Yu et al., 2022), underestimating the need to research the distribution of inhalable bacterial communities (Arellano et al., 2011; Ye et al., 2018). Furthermore, due to droplet evaporation, rain- and snow-induced bacteria could undergo various transformations, including phase transition, pattern formation, and splashing behavior, while overlooking waterborne bacterial communities. Given the numerous urban microbes in the ambient environment, the infections potential of inhalable pathogens in the air is of significant concern (Liu et al., 2022). Thus, datasets are urgently needed to assess exposure risks and the factors influencing the distribution of pathogenic bacterial communities in water and air in urban environments (Belut et al., 2019; Ma et al., 2023).

In this study, we analyze the effects of seasonal precipitation on the transmission risk of environmental microbes in urban settings via, on-site precipitation sampling and high-throughput sequencing techniques. First, this study identified the bacteria community in rainwater and snow. We also assessed the abundance, size distribution, and community structure of atmospheric bioaerosols during extreme precipitation events in spring, summer, autumn, and winter using two Chinese cities as case studies. Second, we ascertained the influencing factors, such as snowmelt water quality parameters and air aerosol concentrations, on bacterial survival. Finally, we conducted an early-warning risk analysis using a health risk assessment of extreme precipitation-induced inhalable bacterial aerosols that affect adults and children.

This study contributes to understanding the transmission dynamics of rain- and snow-borne microbes across urban landscapes.

2. Materials and methods

2.1. Study area

This study collected on-site seasonal snow-/rain-water and air samples from two residential Chinese urban regions. First is the Beijing-Tianjin-Hebei region (TJ site: 39° 4′ N, 117° 8′ E), characterized by a temperate monsoon climate (Fig. S1). It is in the Yanshan Mountain transition zone on the coastal plain, 146 m above sea level. According to the seventh national census in China, the TJ site is in a city with 13.866 million residents over 11,966 km^2 of land area (NBSC, 2021). The city hosts numerous industries, with a gross industrial production value of 1631 billion yuan (TMSBC, 2022).

The second sampling site is located in Fuxin City (FX site: 42° 2′ N, 121° 39′ E), in the western Liaoning area of the northeast plain region of China. It serves as a comparative case. Positioned on the campus of Liaoning Technical University, it is approximately 7 m above sea level and experiences a northern temperate monsoon climate. FX site is in a city with a 1.647 million population, covering 10,445 km^2. The city is known for coal mining and thriving agriculture, with a 58-billion-yuan gross industrial production value (FSBC, 2022). FX is an inland city with meager urbanization and industrialization and lower industrial production and population densities.

Five sets of snow/rain scenarios (No. 1–5) were examined for typical extreme precipitation days in the two cities. All precipitation sampling points were located in urban areas with no significant anthropogenic air pollution sources (industry, agriculture, or construction) in the vicinity.

2.2. Sampling method

2.2.1. Precipitation sampling method

The on-site sampling duration was contingent upon the duration of the extreme precipitation event, and the volume of samples collected correlated with the precipitation intensity. In February 2022, samples from winter extreme atmospheric precipitation and 1–3 d of precipitation were collected every 6–8 h from the onset of snowfall at the TJ site. These samples were categorized into early and late snow precipitation samples (such as, No. 1-snow-TJ). Winter precipitation samples (No. 2-snow-FX) were obtained at the FX site on February 28, 2022. Spring snow samples were collected at the FX site at the beginning, middle, and end of a snowfall (No. 3-snow-FX) on March 14, 2022. During heavy rainfall in summer, precipitation samples (No. 4-rain-TJ) were collected at the TJ site on August 22, 2022. Additionally, autumn precipitation samples were taken in duplicate on October 10, 2022 (No. 5-snow-FX). Detail descriptions of these seasonal samples are listed in Table S1.

Moreover, Table S1 presents warnings of rainstorms or snowstorms.

According to the precipitation intensity, rainstorm warning colors were divided into four levels: blue, yellow, orange, and red. The snow storm yellow warning is standardized as follows: within 12 h, it will snow more than >6 mm, and the snow will continue, which may impact traffic or agriculture and animal husbandry. This study proposes that snowstorms and rainstorms be studied in depth. The warning signals of precipitation color are listed in the supplementary table.

The US Environmental Protection Agency (EPA), recommends a 0.1 L water sample for pathogenic bacterial analysis (*Method 1604–2002*, EPA-821-R-02-024). The Center for Disease Control and Prevention (CDC) advised that a smaller volume is acceptable if 1 L cannot be collected from a source (CDC, 2005). In this study, the volume of precipitation water was determined by the actual scenarios of the 50–1000 mL natural samples. Early detection of bacterial cultures using solid agar plates is cost-effective (Wang et al., 2020). Cultivable bacteria in air and water were detected using this method.

Filter-assisted sequencing and nutrient agar plates were used for analyzing the microbes in the rain-/snow-melt samples (No.1-snow-, No.3-snow-, No.5-snow-samples). During sampling, all experimental instruments (including filter bottles, tweezers, filter membranes, and conical flasks) that contacted the samples were sterilized at 121 °C for 30 min. The collected snow samples were initially placed in 100 mL sterile, sealed sampling bags. These sampling bags were then stored in a sterile incubator at 5 °C. Then, the snow samples were allowed to melt and stand for <12 h before filtering the bacteria through a mixed cellulose sterile membrane (CA, pore size: 0.22 μm, diameter: 47 mm, *Guangdong Huankai Biological Technology Co., Ltd.*) for sequencing, which measured the abundance of live and dead bacteria.

2.2.2. Sample processing and DNA extraction

The DNA preparation step is crucial, necessitating DNA extraction before subsequent experiments. In this study, DNA was extracted from the membrane after capturing bacteria from the snow and rain samples. The membrane was cut into fragments and loaded into 2 mL centrifuge tubes. The DNA extraction kits extracted high-quality bacterial genomic DNA. An Illumina NovaSeq sequencing library was prepared following the manufacturer's instructions, with the relevant absorbance peak examined. Total DNA was extracted as the amplification template, and the bacteria were amplified by polymerase chain reaction (PCR), targeting the 16 S rRNA gene's small fragment. Biological information and data were retrieved from the taxonomy database of the National Center of Biotechnology Information Taxonomy to identify the species and classify the samples.

Further studies on the samples' precipitation-related bacterial abundance, community, and diversity were conducted by sequencing the relevant variable regions of 16 S rDNA. The operational taxonomic units (OTUs)-clustering is a standard procedure obtained by clustering the reads at the 97.0% similarity level using the uSearch software tool. Amplicon sequence variants (ASVs) give an advantage in microbiome analysis. Little information is obtained from ASV-based analysis of precipitation-related microbiome samples with unknown containment levels, as the effects of OUT- or ASV-based analysis results remain unknown (Mokhtari and Ridenhour, 2022).

Principal component analysis (PCA) is one of the most broadly used data mining techniques for grouping samples. In contrast, principal coordinated analysis (PCoA) is a non-binding data dimensionality reduction analysis method. Furthermore, based on relative abundance curves of the bacterial and beta diversity, PCA and PCoA analyses were adopted to compare the similarity in community structures among various samples. To comprehensively assess the alpha diversity and richness of microbial communities, the Shannon index characterized the alpha diversity using Mothur and R software (Shannon, 1948a; Shannon, 1948b).

2.2.3. Airborne bioaerosol sampling method

Andersen impactors sampled airborne bioaerosols during the precipitation events. A six/eight-stage Andersen cascade impactor, designed to measure bacteria's concentration and particle size distribution in ambient air, operated at a 28.3 L/min flow rate. The sampling point was set at a constant height (1.5 m), referring to the average human inhalation height. The total bacterial bioaerosol characteristics and cultivable bacterial species of precipitation events (No. 1–5 snow and rain) in different city sites (TJ, FX) were quantitatively analyzed. Subsequently, the cultivable live bacteria in the precipitation droplets were detected using the initial nutrient agar plates (duplicated), and incubated aerobically at 37 °C for >72 h. Moreover, cultivable pathogenic bacteria in No. 5 snowmelt water samples were detected using a nutrient agar culture medium.

2.2.4. Measuring environmental parameters

Using an air quality detector (*BR-SMART-128S, Bolangtong Medical Technology (Beijing) Co., Ltd.*), airborne particulates with aerodynamic diameters of 1, 2.5, and 10 μm ($PM_{1.0}$, $PM_{2.5}$, and PM_{10}, respectively) were monitored along with the temperature and atmospheric relative humidity. This detector, with a 0–999 μg/m^3 $PM_{2.5}$ measurement range, and ±20 μg/m^3 accuracy, operates within 0–50 °C and 0–90% relative humidity. It features a 6-channel laser emitter, sensors, and software compensator for airborne particulate matter. During extreme winter precipitation events, the concentrations of base cations (Ca^{2+}, Na^{+}, Mg^{2+}, and K^{+}) and pH of snowmelt water samples were analyzed using ion chromatography (*ICP-OES-5110; Aglient Technologies, Inc.*) and a pH meter (*F2-Standard, Mettler Toledo, Inc.*). A digital thermometer and hydrometer (*DPH-103, Kaixingdemao Instrument (Beijing) Co., Ltd.,* Beijing, China) were used during the extreme weather precipitation sampling. Air quality parameters such as SO_2, O_3, NO_2, and air quality index (AQI) were sourced from the meteorological data websites (*aqicn.org/city/tianjin/; aqicn. org/city/fuxin/*).

2.3. Health risk assessment

Inhalation is the primary pathway of human exposure to environmental pollutants (Chen et al., 2021). The exposure concentration of bacteria during extreme precipitation events was measured and calculated using **Eq. (1)**:

$$\mathrm{ADD} = \frac{C_{air} \times \mathrm{IR} \times \mathrm{ET} \times \mathrm{EF} \times \mathrm{ED}}{\mathrm{BW} \times \mathrm{AL}} \quad (1)$$

where ADD represents the average daily dose by inhalation (CFU/kg d), C_{air} denotes the concentration of airborne total bioaerosols (CFU/m^3), ET signifies the inhalation exposure time (assumed to be 24 h/d due to the continuous nature of rain or snow), EF represents the exposure frequency. We used 73 d/yr, reflecting an estimated 64–73 precipitation days. The exposure duration (ED) for adults (30 years) and children (12 years) was considered separately (Oh et al., 2020). The inhalation rate (IR) (Du et al., 2014) is different for adult males (0.8 m^3/h), adult females (0.7 m^3/h) (Chen et al., 2022), and children (0.4 m^3/h) (Kawahara et al., 2011). And with increased physical activity, this rate can be three to six times higher. AL denotes the mean lifespan (77.3 × 365 days), BW represents the mean body weight, based on the Chinese population data (adult males: 61.2 kg, adult females: 56.8 kg, preschool children: 20.0 kg) (Li et al., 2014; Wang et al., 2022). Yet, a unified reference dose (RfD) for airborne bacteria and fungi has not been established (Li et al., 2022).

To estimate health risks via inhalation exposure, the hazard quotient (HQ) and hazard index (HI) were calculated using **Eqs. (2)–(4)**:

$$\mathrm{HQ} = \frac{\mathrm{ADD}}{\mathrm{RfD}} \quad (2)$$

$$\mathrm{RfD} = \frac{\mathrm{RfC} \times \mathrm{IR}}{\mathrm{BW}} \times 24 \quad (3)$$

$$HI = \sum HQ_i \quad (4)$$

where RfD is the reference dose of the airborne bacteria (CFU/m^3) (Xu et al., 2020). The Health and Welfare Department in Canada asserts that 50 CFU/m^3 of any single pathogen species warrants immediate investigation, while 100 CFU/m^3 is considered unacceptable for the presence of other pathogens (Kim et al., 2018). The American Conference of Governmental Industrial Health (ACGIH) suggests that the total culturable bacteria count in indoor air should be < 500 CFU/m^3 (ACGIH, 1986; 1989). The Taiwan Environmental Organisation has recommended an exposure limit of 500 CFU/m^3 for bacteria in indoor air (Kalogerakis et al., 2005; Sadigh et al., 2021). Some studies adopted 500 CFU/m^3 as the RfC to calculate the RfD (CFU/kg d) for assessing airborne bioaerosol pollution (Liang et al., 2023; Zhang et al., 2023). An HI of >1 and.

0–0.5 indicates severe noncarcinogenic and extremely low risk, respectively (Guo et al., 2021).

2.4. Statistical analysis

Analyzing the vast datasets in bioinformatics is challenging. Generating an analysis report from the 16 S rDNA genes sequencing data involves correlation analysis that requires significant time and effort (Miao et al., 2022). We conducted Spearman and Pearson correlation analyses to elucidate detailed correlations between the differential taxa of the most abundant bacterial genera at varying snowfall depths. Furthermore, using a Pearson correlation analysis, the Pearson correlation coefficient (r) gauged the degree of correlation. A *p*-value >0.05 indicates a Gaussian distribution. For clarity, the r-value was categorized into five levels based on its absolute value: 0.9–1 = very strong correlation; 0.7–0.9 = strong correlation; 0.4–0.7 = moderate correlation; 0.2–0.4 = weak correlation; and 0–0.2 = very weak or no correlation.

3. Results and discussion

3.1. Airborne bioaerosol pollution profiles

Bioaerosol concentrations during the winter-autumn period in the two Chinese cities (TJ and FX with different industrial development degrees) were monitored on-site using six-stage bioaerosol samplers. The results revealed the cultivable bioaerosol concentration (C'$_{cb}$) in the outdoor air (Fig. 1a), indicating that C'$_{cb}$ surpassed the reference exposure limit of 500 CFU/m^3. For instance, in the winter precipitation, No. 1-snow at the TJ site exhibited a 591.2 CFU/m^3 C'$_{cb}$, while No. 5-snow at the FX site reached 435.9 CFU/m^3 in autumn precipitation. Notably, in the winter precipitation at TJ, a higher concentration of finer bioaerosols (0.65–1.1 μm) was observed in the air, accounting for 31.3% of the total concentration of bioaerosol. Despite a relatively lower concentration of inhalable finer bioaerosols in the autumn No.5-snow at FX, they accounted for 16.2% of the total bioaerosol concentration. The aerodynamic diameter of individual particulate materials in bioaerosols showed characteristic ranges (0.01–100 μm) (Nazaroff, 2016). These findings suggest that bioaerosols with smaller sizes, which potentially contribute to adverse inhalation impacts (like infectious diseases, allergies, and cancer), are prevalent on snow days.

Furthermore, the spatiotemporal distribution of bioaerosols across six diameter ranges was analyzed over the winter snow period (Fig. 1b). In No. 1-snow-TJ (February 13, 2022), airborne bioaerosols were monitored in-situ and analyzed throughout the storm snow. Snow samples deserve a measurement of the precipitation duration, here, six-time points were selected: T1 (snow, 0.5 h), T2 (snow, 12 h), T3 (snow, 18 h), T4 (snow, 24 h), T5 (post-snowfall, 8 h), and T6 (post-snowfall, 56 h). At T1, bioaerosols constituted 57% of the total concentration, with those in the 0.65–3.3 μm range peaking at 1731 CFU/m^3 (a sum of

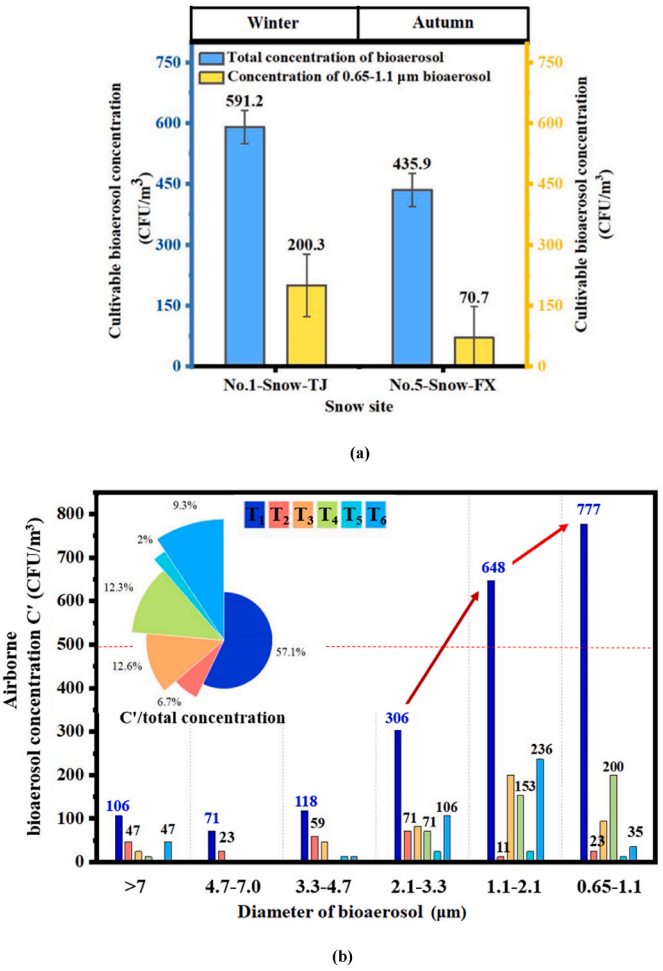

Fig. 1. Airborne transported bioaerosol characteristics during seasonal precipitations. a) Concentration of airborne cultivable bacteria bioaerosols during winter/autumn seasonal precipitation (No. 1-snow-TJ and No. 5-snow-FX). b) Airborne bioaerosol concentrations during six sampling in a winter snowstorm (No. 1-snow-TJ).

the right three blue columns with red arrows in Fig. 1b). At T4, the concentration of 0.65–3.3 μm bioaerosols decreased by 75.5%, and the 1.1–2.1 μm bioaerosols reached a relatively high value of 153 CFU/m^3 at T4. At T6, the 1.1–2.1 μm bioaerosols peaked at 236 CFU/m^3. From T1 to T6 during the snow, the airborne bioaerosol concentration ratio dropped to its lowest (2%) at T5, and then increased approximately fourfold (9%) by T6. These results demonstrate that the concentration distribution of abundant fine bioaerosols in the air, including those with <1 μm diameters, varied temporally with changes in winter precipitation intensity, and duration.

Compared with the high bioaerosol concentrations during the snowstorms in TJ city (No.1-snow), one-year on-site observation of bioaerosol concentration in the 2023 year further demonstrated that bioaerosol concentrations were relatively low in winter, with significant spatiotemporal differences during seasonal precipitation events in FX city. The mean concentration ranges of airborne bioaerosols in winter, summer, autumn precipitations reached 106–169, 75–710, and 605–1290 CFU/m^3. There was >500 CFU/m^3 bioaerosol pollution during the rainy days in the autumn but much lower during the snowy winter days. Then, the samples urged further research on the varied bioaerosol emissions in the precipitation events of seasonal polluted days in cities during the eco-city's construction.

3.2. Winter precipitation-triggered dominant bacteria

To study the bacterial distribution during snow episodes, we analyzed the bacterial community structures and diversity in rainwater/snowmelt (Fig. S1b-c and S2). Early and late snowfall samples (No. 1-snow-TJ: T2 and T4) were pre-processed, and the raw data were spliced and dechimerized by *Barcode*, producing 12,921 sequences. Each sample yielded at least 5450 CCS sequences, with a mean of 6461 sequences. The OTU analysis indicated bacterial richness and diversity (Fig. S1b). A sharp increase in the OTU curves reflected a high taxa presence in bacterial communities, suggesting sample species richness (Lladó Fernández et al., 2019). The flattening OTU curve indicated species numbers insignificantly change with more sequencing cycles, suggesting sufficient sample sequencing for data analysis (Fang et al., 2023).

The Shannon index (H) assessed microbial evolution in extreme precipitation environments. The H curve, which quantifies microbial species diversity in a sample (Fig. S1c), was flat, and the number of sequences was sufficiently large to represent the microbial species. The wider the H curve, the richer the species composition. The Shannon index at T2 (500 sample numbers) was 5.6 and, increased to 6.4 at T4, suggesting a richer composition of bacterial species in the snowmelt as snowfall time progressed. At a 500-sample number, early snowfall (12 and 24 h) had 77 and 125 OTUs, respectively. The snow samples revealed a high species count as snow accumulated. For example, at a sample population of 1,375, the 12- and 24-h snow had 87 and 156 OUTs, respectively (Fig. S2).

At the beginning of snowfall, the bacterial groups in the snow samples were abundant, i.e., Streptococcus, Staphylococcus, and Veillonella, with 21.6%, 11.4%, and 13.1% abundance, respectively (totaling 46.1%) (Fig. 2). These species, prevalent in the human gut and saliva system, can survive in cold environments (Shu and Huang, 2022), suggesting heterogeneous snow origins. At the end of snowfall (T4), Carnobacterium, Methylobacterium, and Arthrobacter showed a relative abundance of >8.9%, >6.4%, and >6.2%, respectively (totaling 21.5%). Cultivable pathogens like *Streptococcus pneumoniae*, *Staphylococcus epidermidis*, and *Escherichia coli* (Table S2), exist in air and precipitation water and have the highest relative abundance.

A phylogenetic tree summarized the kinship among species in the winter snow sample (No. 1-snow-TJ) (Figs. S2a–b). The 16 S rRNA genes sequences were grouped into two: Firmicutes and Proteobacteria. Gammaproteobacteria, Pseudomonadales, Proteobacteria, Alphaproteobacteria, and Lactobacillales were widely distributed in the snow at various times, with Bacillus distinctly present in the 24-h snow sample. The 12-h snow sample had unique Kallotenuales, Lactobacillaceae, Beijerinckiaceae, Hyphomicrobium, and Rubellimicrobium species, while those of 24-h had distinctive Bacilli species, i.e., Abiotrophia, Granulicatella, Negativicutes, Methylocella, and Stenotrophomonas. These sequences demonstrated the significance of changes in the distribution of bacterial communities in snowmelt during extreme precipitation. Furthermore, Aerococcus, Cyanobacteria, Carnobacterium, Streptococcus, Clostridia, Paracoccus, Rickettsiales, Sphingomonas, Acinetobacter, Enhydrobacter, Psychrobacter, and Pseudomonas were related. Psychrotolerant Cyanobacteria and proteobacterial abundance patterns were consistent with those reported in ice sheets, while cyanobacterial extracellular polysaccharides contributed to the aggregation of surviving granules, such as microbe-mineral aggregates (Anesio et al., 2017). Moreover, during winter precipitation at the TJ site, airborne cultivable bacteria (like *Streptococcus pneumonia* (*Pneumococcus*), *Escherichia coli*, *Bacillus cereus*, *Staphylococcus aureus*, and *Staphylococcus epidemidis*, and *Staphylococcus*) were prevalent in the urban near-surface atmosphere (Table S2). Moreover, many bacteria evinced inexact sequencing information.

3.3. Bacterial community variation during seasonal precipitation

Bacterial diversity increases under low-temperature precipitation in monsoon climates (Ren et al., 2020). Consequently, ambient variations in bacterial communities during precipitation were significant in our study. Beyond investigating No. 1-snowfalls-TJ, we also examined other seasonal precipitation events. For instance, samples No. 2–4, encompassing snow and rain, were assessed during four seasonal precipitation periods at FX and TJ. No. 3-snow involved investigations at three distinct snowfall time points: T_i (snow depth 0–4 mm), T_m (snow depth 4–6 mm), and T_e (snow depth 6–10 mm).

Upon identifying the bacterial species present in the snow, we found that the marine bacterium Pseudomonas was the most abundant, constituting 64% of the total Fig. 3. Additionally, the abundance of Massilia and Arthrobacter (typically found in soils), increased with snowfall event No. 3 duration. The genera Pseudomonas, Sphingomonas, Pedobacter, Arthrobacter, Brevundimonas, Flavobacterium, Chryseobacterium, Variovorax, Aeromicrobium, and Roseomonas were the dominant species in the spring snowmelt samples of No. 3-snow-FX. At the end of the snowfall period (T_e), the abundance of Pseudomonas increased further, with a notable rise in the relative abundance of Arthrobacter, Flavobacterium, and Massilia. Moreover, Pseudomonas is a widely distributed pathogen in the environment, capable of infecting humans and plants, thus affecting local water and life cycles (De Smet et al., 2017; Xin et al., 2018).

In Fig. S3a, at the genus level, the predominant bacterial genera comprised common microbial genera, including Pseudomonas, Massilia, and Pedobacter. The distribution of the most abundant bacterial genera at two different precipitation events is illustrated using PCoA analysis (Fig. S3b). Four symbols represent the differences in bacterial species of

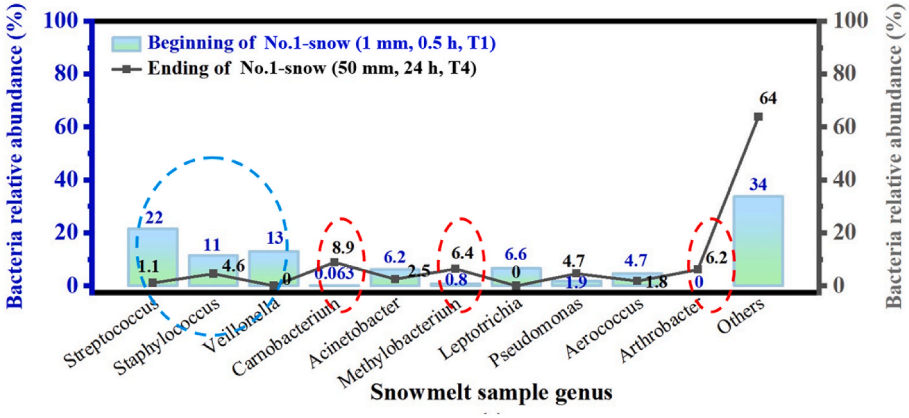

Fig. 2. Snow-originated bacteria relative abundance profiles of snowmelt in a whole snow episode.

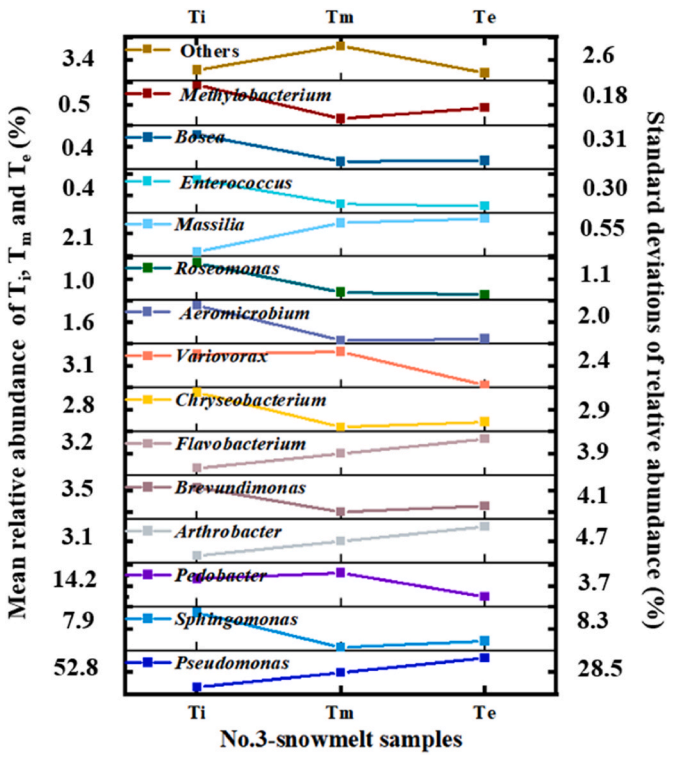

Fig. 3. Bacteria abundance changes in T_i, T_m, T_e of No. 3-snow in FX (spring).

four snowmelt water samples. The shorter projection distance suggests variations in microbial compositions during the long-duration, 50 mm-depth precipitation. The analysis demonstrated that bacterial genera between winter- and spring-snow water samples had different community compositions.

The dominant microbial processes in natural rain- and snow-bacterial communities are influenced by location, season, and snowfall depth and duration (Liu et al., 2018; Smirnova et al., 2021). This variability was evident in the bacterial community analyses conducted at the two sites. During the storm snow period (No. 2-snow), Pseudomonas and Pedobacter were abundant in the snow, constituting 35.6% and 29.2% of the taxa, respectively (Fig. S4a). In the spring snow samples (No. 3-snow) from the FX site, these two bacterial genera had a relative proportion of 59.8% and 14.3%, respectively (Fig. S4b). However, in the summer rainwater samples (No. 4-rain), their proportion was 38.3% and 25%, respectively. Additionally, Massilia was abundant (18%) in the summer rain samples (No. 4-rain; August 22, 2022) (Fig. S4c). These findings further suggest that the composition of pathogenic bacterial communities in seasonal precipitation varies among industrial cities. However, the contribution of these predominant genera was consistently significant across the scenarios.

The post-snowfall increase in the relative abundance of cold-tolerant bacterial taxa highlights how the composition of bacterial species significantly varies with the precipitation type, be it snowfall or rainfall. Notably, the most remarkable diversity in bacterial taxa was observed during the spring snowfalls. This variation is evident from the taxa analysis of the seasonal precipitation water samples from winter and spring. A percent stacked column chart illustrates the relative abundances of the 30 most abundant taxa (Fig. S4d). In No. 2-snow and No. 3-snow samples, Pseudomonas showed substantial relative abundance of 40% and 60%, respectively. This prevalence is attributed to the diverse roles of Pseudomonas genera within the microbial community, functioning as pathogens, epiphytes, and ice nuclei in the atmospheric environment. Furthermore, the relative abundance of Bradyrhizobium and Massilia was notably high, exceeding 85% (98% and 89%, respectively) in No. 2-snow. In contrast, Chryseobacterium, Brevundimonas, Flavobacterium, and Nocardioides exhibited the highest relative abundance in No. 3-snow, each reaching 100%. These findings underscore the dynamic nature of snow microbial communities. The observed patterns align excellently with previous findings (Peiffer et al., 2021).

Our dominant bacterial community analysis revealed a notable sensitivity in bacterial composition and abundance to snowfall duration. This sensitivity was particularly evident when examining the eight most abundant bacterial genera in the No. 1-snow-melt water at varying depths. Specific genera were distinct for their prevalence in snowmelt water at 10 mm and 20 mm depths (Table S3). Notably, Streptococcus and Staphylococcus were more common genera at higher snow depths, while Carnobacterium was prevalent at lower snow depths, indicating a higher risk during the preliminary snow stage.

In summary, longer bioprecipitation duration dominated the predominance Pseudomonas' relative abundance across all study's four seasonal precipitation events. The correlation of bacterial abundance and taxa with the snow period, suggests a potential link with increased Pseudomonas infections. Despite the lack of precise sequence information, detecting many new microbial species indicates a rich and diverse microbial presence in these environments. However, this diversity also raises concerns, especially regarding the abundance of gram-negative bacteria and the transmission of endotoxins capable of causing significant public health problems. Therefore, we further analyzed the dominant bacterial abundance and community variation, including Pseudomonas during snow periods.

3.4. Dominant bacteria correlation analysis

A biomedical statistical correlation analysis was conducted to comprehensively investigate the factors influencing snow bacterial communities and health risk profiles. The 18 most abundant OTUs of bacterial genera (partial) observed in No. 3-snow (spring) and No. 4-rain (summer) were identified (Table S4). During the snow period, taxonomic data exhibited high correlations (Fig. S5a). However, the correlation coefficient for abundance indicated a weak or negative relationship ($r = 0.34$ or $r = -0.28$), suggesting that among the bacterial genera, Pseudomonas had a strong correlation ($r = 0.81$) with Acinetobacter (Fig. S5b).

Moreover, Acinetobacter strongly correlated ($r = 0.99$) with Streptococcus and Aerococcus. These three bacteria correlated negatively with a high abundance of the predominant Carnobacterium, implying that Aerococcus, Streptococcus, and Acinetobacter may inhibit forming predominant bacteria. Pseudomonas positively associated significantly with five other dominant bacteria. This association indicates that the growth of the most abundant bacterium (Pseudomonas), was promoted in the three precipitation events.

The analysis also revealed that the correlation grade of the taxon values in No. 4-rain and No. 3-snow at the T_i time point was extremely high ($r = 0.90$) (Fig. S5c). Snow and rain samples exhibited strong and moderate correlations, respectively ($r > 0.40$). Moreover, the four seasonal precipitation (snow/rainwater) samples showed varied correlations with taxon information. Therefore, the influence of multiple environmental parameters on the ambient bacterial community, abundance, and the risks posed by strongly correlated pathogens with dominant bacteria, such as Pseudomonas, warranted further investigation.

3.5. Factors influencing variations in bacterial communities

Variations in airborne particulate levels are often attributed to weather patterns, such as a stable atmosphere (Jung et al., 2019). However, the contribution of meteorological conditions and air quality parameters to bacterial communities in aerosols during extreme precipitation events remains unclear (Ouyang et al., 2020). This study provides comparative profiles of the concentration of cultivable bioaerosol, and fine particulate matter in air. Focusing on No.1 snow as a

case study, air quality parameters were measured at the T1-T6 snow time points on February 12, 2022 (Fig. 4a). During a severe particulate pollution episode, transient $PM_{2.5}$ concentrations exceeding 100 μg/m^3 were observed at the TJ site, throughout the snowy winter. This study found that the population of cultivable bacteria in the air increased with the airborne fine particulate concentration, suggesting increased airborne biological particulates throughout the snowfall.

The concentration of some principal air pollutants, notably NO_2, generally declined during the COVID-19 lockdowns (Shen et al., 2022). During this study, the atmospheric concentration of SO_2 and NO_2 was as low as 7 and 27 μg/m^3, respectively (Table S5). Moreover, the AQI decreased similarly to the bioaerosol concentrations from T1 to T6.

Moreover, as snowfall accumulated, the pH and cation mass concentration of snowmelt water decreased notably, corresponding to a lower concentration of cultivable bacteria (Fig. 4b). For instance, the pH of snowpacks decreased with depth, i.e., 7.49, 7.28, and 7.25 at 0–10 mm, 10–35 mm and 35–50 mm, respectively. Similarly, the toxicity of cations, such as Mg^{2+} and Ca^{2+}, significantly impacts microbial activity in biological wastewater treatments and alters microbial structures (Macêdo et al., 2019). In this study, the concentrations of the four base cations (Ca^{2+}, Na^+, Mg^{2+}, and K^+) varied temporally. For example, the cumulative cation concentration in the snowpack at 10–35 mm was 2.56-, 2.02-, 2.31-, and 1.20-times higher than those at 35–50 mm, respectively. These decreasing concentration gradients of cations and H^+ can influence the diversity and significant variations in the bacterial community composition toward the end of extreme precipitation events. These findings suggest that anthropogenically emitted cations impact precipitation-propagated (airborne or waterborne) bacterial communities in urban hydrological cycles.

Culture-based detection of cultivable inhalable bacteria induced by seasonal precipitation is crucial for understanding the spatiotemporal distribution of pathogens. Aside from the cultivable bioaerosols in the air, this study detected the cultivable bacteria in precipitation water. For example, in FX city, the predominant bacteria in snowmelt sample No. 3 were primarily human pathogenic Bacillus bacteria, such as *Staphylococcus aureus MRSN 8611* and *Staphylococcus aureus* (Table S6 and Fig. S6). In contrast, snow sample No. 5 predominantly contained probiotics such as *Bacillus subtilis* and *Bacillus amyloliquefaciens*. These probiotics can inhibit pathogenic microorganisms that damage organs via infections (Table S7). These findings confirm that various biological precipitation events occur in different seasons. Therefore, the information on cultivable bacteria during spring precipitation is significant, as it impacts the pathogenic bacterial community, activity, concentration, and infection potential (Zeng and An, 2021); thus, it warrants further research attention.

3.6. Assessment human health risk

This section assesses the human health impacts of most bacteria in water and air (diffused) biological compounds during precipitation, focusing on snow/rain-accompanied bioaerosols. These rainstorm/snowstorm event-related bioaerosol exposure analyses, were based on the on-site measured bioaerosol concentration in the extreme precipitations. They highlighted the adverse health effects of unexpected bioaerosol exposure and health risks in outdoor city environment. Comparing the inhalation exposures for male adults, female adults, and children, we found that the time-averaged mean inhalation risk (HQ; 0.093 at T1–T6) for male adults showed an inhalation exposure of 29% of the maximum HQ of T1, 0.32 at 0.5 h in to the snowfall (Fig. 5). In comparison, the time-averaged HQ values (0.085 at T1–T6) for female adults decreased to 9%, with the maximum HQ at T1 (0.29 at 0.5 h into the snowfall) dropping to 10%. For children, the mean HQ value was 0.011 at T1–T6, equaling 12% of that of adult males (T1 to T6), while the maximum HQ at T1 (0.0375) was 2.4 times higher. These findings indicate that the mean HQ of airborne bioaerosol exposure in adults is higher than in preschool children during precipitation. The bioaerosol

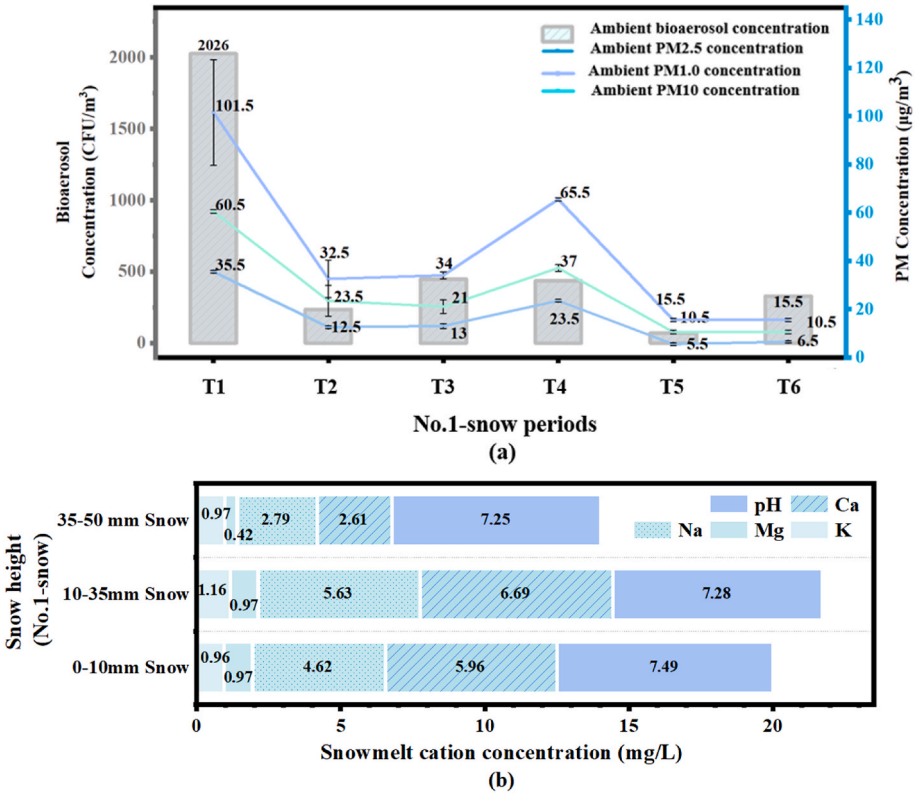

Fig. 4. Airborne bioaerosol concentration interactions with meteorological and weather factors. a) PM concentration. b) Base cation concentration and pH at 0–50 mm snow depth.

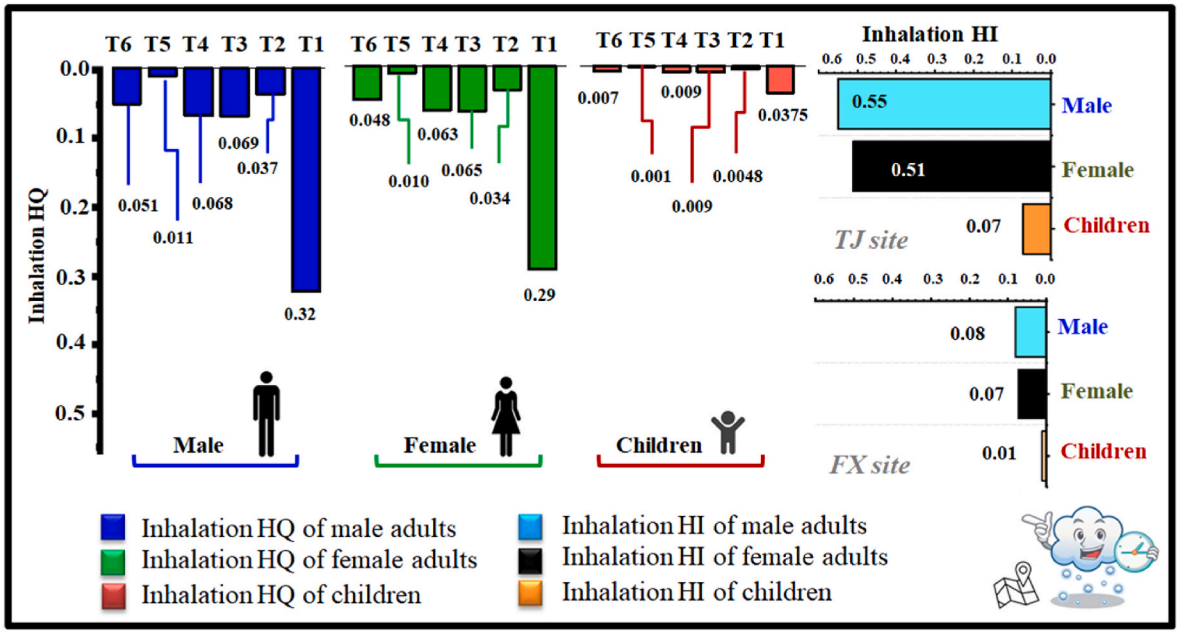

Fig. 5. Health risks related to seasonal extreme precipitation events for male adults, female adults, and children during outdoor activities.

composition (such as 1.0 μm particulate matter carrying Pseudomonas) may further enhance the infection potential. The HQs for adult males, females, and children showed significant temporal differences during the initial precipitation phase. This variation is primarily due to the higher inhalation rate in males, resulting in a correspondingly higher HQ. However, when the ratio of inhalation rate to body weight increases, as seen with higher inhalation rates induced by strenuous exercise, female adults and children may experience high HQ risk.

Furthermore, we investigate the bioaerosol exposure and air particulate pollution during precipitation in the two cities. The highest HI for males was in TJ during winter precipitation (No. 1-snow), coinciding with high $PM_{2.5}$ concentrations (63 μg/m^3). In contrast, the HI decreased by 85% during autumn precipitation (No. 5-snow) in FX, where lower $PM_{2.5}$ concentrations (3 μg/m^3) were observed. This result indicates that spatial-temporal variations in seasonal precipitation can lead to diverse particulate exposure risk, especially during dense particulate pollution associated with precipitation. The monitored PM concentration is a crucial indicator of the degree of precipitation linked to a higher abundance of environmental pathogen pollution. For instance, on days with seasonal precipitation in areas with heavy industrial activity and dense populations (such as the TJ City), higher concentrations of micrometer- and nanometer-sized PM carrying more cultivable opportunistic bacteria are dispersed in the urban near-surface atmosphere.

Moreover, in 2023, we also quantified seasonal precipitation ions, bioaerosols, particulate matter/aerosols ($PM_{1.0}$, $PM_{2.5}$, and PM_{10}), and other parameters in the precipitation days. A similar case of higher aerosol concentration in the early hours of the snowstorm periods, such as a snowstorm on November 6, 2023, was observed. In the early snowstorm period at FX, airborne $PM_{1.0}$, $PM_{2.5}$, and PM_{10} concentrations reached 40, 65, 109 μg/m^3, respectively, while those concentrations reached 1, 3, 6 μg/m^3. However, bioaerosol concentration was not excessively high, demonstrating variations of aerosol pollutants in extreme precipitation durations. Moreover, at TJ, the NO_3^- and SO_4^{2-} concentrations (5.23 and 4.44 mg/L, respectively) were about seven and five times those of the representative anions' concentration (0.85 and 0.59 mg/L, respectively) of FX rainstorm water. These values demonstrated the differences in the precipitation water composition from various industrial cities. Consequently, precautions are necessary during biological precipitation extremes to mitigate unexpected inhalation exposure and infection.

4. Conclusions

This study explored the impact of extreme precipitation events on disseminating microbes in the urban environment and assessed potential health risks. The gram-negative bacterium Pseudomonas was highly abundant in rainwater and snowmelt samples. Pseudomonas, Methylobacterium, Staphylococcus, Acinetobacter, Massilia, Aeromonas, Streptococcus, Veillonococcus, and Bosea predominated the bacterial communities in these samples. We confirmed that infectious, partially cultivable bacteria present in the air, such as *Escherichia coli*, *Staphylococcus epidemidis*, and *Streptococcus pneumonia* (*Pneumococcus*), were dispersed during winter snow events. These bacteria were transported by inhalable bioaerosols (0.65–3.3 μm in diameter), potentially increasing inhalation risk (HI = 0.55, male). Typically, during the snow storm events in FX, the risk of bioaerosol inhalation was lower (HI = 0.08 for males). Furthermore, the inhalation risk for adults was four times higher in TJ (e.g., T1: HQ: 0.32 for males, 0.29 for females; T4: HQ: 0.068 for males, 0.063 for females). Therefore, appropriate prewarming about the elevated infection risk of particulate matter laden with pathogenic bacteria in urban outdoor hydrological environments are warranted. This study underscores the spatiotemporal differences in bacterial community distributions and the unexpected pathogen exposure risks in outdoor spaces of various industrial cities, indicating the need for further research in this area.

CRediT authorship contribution statement

Ting Zhang: Conceptualization, Investigation, Validation, and Writing – original draft. **Dingqiang Zhang:** Methodology, Data curation. **Zhonghang Lyu:** Methodology. **Jitao Zhang:** Methodology. **Xian Wu:** Methodology. **Yingxin Yu:** Writing – review & editing.

Declaration of competing interest

The authors declare that they have no known competing financial interests or personal relationships that could have appeared to influence the work reported in this paper.

Data availability

Data will be made available on request.

Acknowledgement

The work was financially supported by the National Natural Science Foundation of China (42007385 and 42130611), Guangdong Provincial Key R&D Program (2022-GDUT-A0007), Guangdong-Hong Kong-Macao Joint Laboratory for Contaminants Exposure and Health (2020B1212030008), Liaoning Provincial Natural Science Foundation of China (2023-MS-316) and the Doctor Project of Liaoning Technical University (21–1144).

Appendix A. Supplementary data

Supplementary data to this article can be found online at https://doi.org/10.1016/j.envpol.2024.123406.

References

Anesio, A.M., Lutz, S., Chrismas, N.A.M., Benning, L.G., 2017. The microbiome of glaciers and ice sheets. npj Biofilms and Microbiomes 3, 10.
ACGIH, 1986. Guidelines for Assessment of Bioaerosols in the Indoor Environment. American Conference of Governmental Industrial Hygienists, Cincinnati.
ACGIH, 1989. Guidelines for Assessment of Bioaerosols in the Indoor Environment. American Conference of Governmental Industrial Hygienists, Cincinnati.
Antony, R., Sanyal, A., Kapse, N., Dhakephalkar, P.K., Thamban, M., Nair, S., 2016. Microbial communities associated with Antarctic snow pack and their biogeochemical implications. Microbiol. Res. 192, 192–202.
Arellano, L., Fernández, P., Tatosova, J., Stuchlik, E., Grimalt, J.O., 2011. Long-range transported atmospheric pollutants in snowpacks accumulated at different Altitudes in the Tatra Mountains (Slovakia). Environ. Sci. Technol. 45, 9268–9275.
Behrangi, A., Christensen, M., Richardson, M., Lebsock, M., Stephens, G., Huffman, G.J., Bolvin, D., Adler, R.F., Gardner, A., Lambrigtsen, B., Fetzer, E., 2016. Status of high-latitude precipitation estimates from observations and reanalyses. J. Geophys. Res. Atmos. 121, 4468–4486.
Belut, E., Sánchez Jiménez, A., Meyer-Plath, A., Koivisto, A.J., Koponen, I.K., Jensen, A. C.Ø., MacCalman, L., Tuinman, I., Fransman, W., Domat, M., Bivolarova, M., van Tongeren, M., 2019. Indoor dispersion of airborne nano and fine particles: main factors affecting spatial and temporal distribution in the frame of exposure modeling. Indoor Air 29, 803–816.
Cariñanos, P., Foyo-Moreno, I., Alados, I., Guerrero-Rascado, J.L., Ruiz-Peñuela, S., Titos, G., Cazorla, A., Alados-Arboledas, L., Díaz de la Guardia, C., 2021. Bioaerosols in urban environments: trends and interactions with pollutants and meteorological variables based on quasi-climatological series. J. Environ. Manag. 282, 111963.
Centers for Disease Control and Prevention (CDC), 2005. CDC Laboratory Guidance for Processing Environmental Samples.
Chemke, R., Ming, Y., Yuval, J., 2022. The intensification of winter mid-latitude storm tracks in the Southern Hemisphere. Nat. Clim. Change 12, 553–557.
Chen, D., Liu, R., Lin, Q., Ma, S., Li, G., Yu, Y., Zhang, C., An, T., 2021. Volatile organic compounds in an e-waste dismantling region: from spatial-seasonal variation to human health impact. Chemosphere 275, 130022.
Chen, X., Ward, T.J., Sarkar, C., Ho, K.-F., Webster, C., 2022. Health risks of adults in Hong Kong related to inhalation of particle-bound heavy metal(loid)s. Air Quality, Atmosphere & Health 15, 691–706.
De Smet, J., Hendrix, H., Blasdel, B.G., Danis-Wlodarczyk, K., Lavigne, R., 2017. Pseudomonas predators: understanding and exploiting phage–host interactions. Nat. Rev. Microbiol. 15, 517–530.
Dean, K., Mitchell, J., 2020. A dose response model for the inhalation route of exposure to P. aeruginosa. Microbial Risk Analysis 15, 100115.
Dreier, M., Meola, M., Berthoud, H., Shani, N., Wechsler, D., Junier, P., 2022. High-throughput qPCR and 16S rRNA gene amplicon sequencing as complementary methods for the investigation of the cheese microbiota. BMC Microbiol. 22, 48.
Du, Z., Mo, J., Zhang, Y., 2014. Risk assessment of population inhalation exposure to volatile organic compounds and carbonyls in urban China. Environ. Int. 73, 33–45.
Failor, K.C., Schmale, D.G., Vinatzer, B.A., Monteil, C.L., Monteil, C.L., Monteil, C.L., 2017. Ice nucleation active bacteria in precipitation are genetically diverse and nucleate ice by employing different mechanisms. ISME J. 11, 2740–2753.
Fang, F.-Z., Chen, S.-L., Gui, H.-Y., Li, Z.-J., Zhang, X.-F., 2023. Long-read sequencing analysis revealed the impact of forest conversion on soil fungal diversity in limu mountain, hainan. Microb. Ecol. 86, 872–886.
Fuxin Statistics Bureau, China (FSBC), 2022. Fuxin City Regional GDP Unified Accounting Report.
Georgescu, M.R., Broadbent, A.M., Wang, M., Krayenhoff, E.S., Moustaoui, M., 2021. Precipitation response to climate change and urban development over the continental United States. Environ. Res. Lett. 16.
Guo, K., Qian, H., Ye, J., Sun, F., Zhuge, Y., Wang, S., Liu, C., Cao, G., Zheng, X., 2021. Assessment of airborne bacteria and fungi in different-type buildings in Nanjing, a hot summer and cold winter moist Chinese city. Build. Environ. 205, 108258.
Haas, D., Kriso, A., Fritz, T., Galler, H., Habib, J., Ilieva, M., Kropsch, M., Ofner-Kopeinig, P., Stonitsch, M., Strasser, A., Zentner, E., Reinthaler, F.F., 2020. Background concentrations of cultivable, mesophilic bacteria and dust particles in the air in urban, rural and mountain regions. Int. J. Environ. Res. Publ. Health 17, 9572.
Hemmati, M., Kornhuber, K., Kruczkiewicz, A., 2022. Enhanced urban adaptation efforts needed to counter rising extreme rainfall risks. npj Urban Sustainability 2, 16.
Hu, K., Chen, G., Gregory-Eaves, I., Huang, L., Chen, X., Liu, Y., Leavitt, P.R., 2019. Hydrological fluctuations modulate phototrophic responses to nutrient fertilization in a large and shallow lake of Southwest China. Aquat. Sci. 81, 37.
Hu, W., Wang, Z., Huang, S., Ren, L., Yue, S., Li, P., Xie, Q., Zhao, W., Wei, L., Ren, H., Wu, L., Deng, J., Fu, P., 2020. Biological aerosol particles in polluted regions. Current Pollution Reports 6, 65–89.
Huang, S., Hu, W., Chen, J., Wu, Z., Zhang, D., Fu, P., 2021. Overview of biological ice nucleating particles in the atmosphere. Environ. Int. 146, 106197.
Jeznach, L.C., Hagemann, M., Park, M.-H., Tobiason, J.E., 2017. Proactive modeling of water quality impacts of extreme precipitation events in a drinking water reservoir. J. Environ. Manag. 201, 241–251.
Joung, Y.S., Ge, Z., Buie, C.R., 2017. Bioaerosol generation by raindrops on soil. Nat. Commun. 8, 14668.
Jung, M.-I., Son, S.-W., Kim, H.C., Kim, S.-W., Park, R.J., Chen, D., 2019. Contrasting synoptic weather patterns between non-dust high particulate matter events and Asian dust events in Seoul, South Korea. Atmos. Environ. 214, 116864.
Kalogerakis, N., Paschali, D., Lekaditis, V., Pantidou, A., Eleftheriadis, K., Lazaridis, M., 2005. Indoor air quality—bioaerosol measurements in domestic and office premises. J. Aerosol Sci. 36, 751–761.
Kawahara, J., Tanaka, S., Tanaka, C., Aoki, Y., Yonemoto, J., 2011. Estimation of daily inhalation rate in preschool children using a tri-axial accelerometer: a pilot study. Sci. Total Environ. 409, 3073–3077.
Kim, K.-H., Kabir, E., Jahan, S.A., 2018. Airborne bioaerosols and their impact on human health. J. Environ. Sci. 67, 23–35.
Lei, C., Yu, Z., Sun, X., Wang, Y., Yuan, J., Wang, Q., Han, L., Xu, Y., 2023. Urbanization effects on intensifying extreme precipitation in the rapidly urbanized Tai Lake Plain in East China. Urban Clim. 47, 101399.
Li, Y., Yang, L., Song, H., Ba, Y., Li, L., Hong, Q., Wang, Y., 2022. The changing pattern of bioaerosol characteristics, source and risk under diversity brush aerator speed. Ecotoxicol. Environ. Saf. 236, 113478.
Li, Y., Zheng, L., Xi, H., Yu, K., Lu, S., Tian, J., Song, X., Bao, J., Li, Y., Zhang, X., Wen, Y., Ren, F., 2014. Body weights in Han Chinese populations. Chin. Sci. Bull. 59, 5096–5101.
Liang, Z., Yu, Y., Wang, X., Liao, W., Li, G., An, T., 2023. The exposure risks associated with pathogens and antibiotic resistance genes in bioaerosol from municipal landfill and surrounding area. J. Environ. Sci. 129, 90–103.
Liu, K., Liu, Y., Hu, A., Wang, F., Zhang, Z., Yan, Q., Ji, M., Vick-Majors, T.J., 2021. Fate of glacier surface snow-originating bacteria in the glacier-fed hydrologic continuums. Environ. Microbiol. 23, 6450–6462.
Liu, W., Allison, S.D., Li, P., Wang, J., Chen, D., Wang, Z., Yang, S., Diao, L., Wang, B., Liu, L., 2018. The effects of increased snow depth on plant and microbial biomass and community composition along a precipitation gradient in temperate steppes. Soil Biol. Biochem. 124, 134–141.
Liu, Y., Ji, M., Yu, T., Zaugg, J., Anesio, A.M., Zhang, Z., Hu, S., Hugenholtz, P., Liu, K., Liu, P., Chen, Y., Luo, Y., Yao, T., 2022. A genome and gene catalog of glacier microbiomes. Nat. Biotechnol. 40, 1341–1348.
Liu, Y., Yao, T., Kang, S., Jiao, N., Zeng, Y., Shi, Y., Luo, T., Jing, Z., Huang, S., 2006. Seasonal variation of snow microbial community structure in the East Rongbuk glacier, Mt. Everest. Chin. Sci. Bull. 51, 1476–1486.
Lladó Fernández, S., Větrovský, T., Baldrian, P., 2019. The concept of operational taxonomic units revisited: genomes of bacteria that are regarded as closely related are often highly dissimilar. Folia Microbiol. 64, 19–23.
Lou, M., Liu, S., Gu, C., Hu, H., Tang, Z., Zhang, Y., Xu, C., Li, F., 2021. The bioaerosols emitted from toilet and wastewater treatment plant: a literature review. Environ. Sci. Pollut. Res. Int. 28, 2509–2521.
Ma, L., Yabo, S.D., Lu, L., Jiang, J., Meng, F., Qi, H., 2023. Seasonal variation characteristics of inhalable bacteria in bioaerosols and antibiotic resistance genes in Harbin. J. Hazard Mater. 446, 130597.
Macêdo, W.V., Sakamoto, I.K., Azevedo, E.B., Damianovic, M.H.R.Z., 2019. The effect of cations (Na+, Mg2+, and Ca2+) on the activity and structure of nitrifying and denitrifying bacterial communities. Sci. Total Environ. 679, 279–287.
Madakumbura, G.D., Thackeray, C.W., Norris, J., Goldenson, N., Hall, A., 2021. Anthropogenic influence on extreme precipitation over global land areas seen in multiple observational datasets. Nat. Commun. 12, 3944.
Mardonova, M., Han, Y.-S., 2023. Environmental, hydrological, and social impacts of coal and nonmetal minerals mining operations. J. Environ. Manag. 332, 117387.
Miao, S.-M., Xia, Y., Cui, J.-L., Wang, J.-H., Wang, M.-L., 2022. Correlation analysis between differential metabolites and bacterial endophytes of Ephedra sinica in different years. Ind. Crop. Prod. 175, 114250.
Mokhtari, E.B., Ridenhour, B.J., 2022. Filtering ASVs/OTUs via mutual information-based microbiome network analysis. BMC Bioinf. 23, 380.
Monteil, C.L., Bardin, M., Morris, C.E., 2014. Features of air masses associated with the deposition of Pseudomonas syringae and Botrytis cinerea by rain and snowfall. ISME J. 8, 2290–2304.
National Bureau of Statistics of China (NBSC), 2021. China Statistical Yearbook: the National Bureau of Statistics of the People's republic of China.
Nazaroff, W.W., 2016. Indoor bioaerosol dynamics. Indoor Air 26, 61–78.
O'Connor, D.J., Daly, S.M., Sodeau, J.R., 2015. On-line monitoring of airborne bioaerosols released from a composting/green waste site. Waste Manag. 42, 23–30.

Oh, H.-J., Ma, Y., Kim, J., 2020. Human inhalation exposure to aerosol and health effect: aerosol monitoring and modelling regional deposited doses. Int. J. Environ. Res. Publ. Health 17, 1923.
Ouyang, W., Gao, B., Cheng, H., Zhang, L., Wang, Y., Lin, C., Chen, J., 2020. Airborne bacterial communities and antibiotic resistance gene dynamics in PM2.5 during rainfall. Environ. Int. 134, 105318.
Park, C., Kim, S.B., Choi, S.H., Kim, S., 2021. Comparison of 16S rRNA gene based microbial profiling using five next-generation sequencers and various primers. Front. Microbiol. 12.
Peiffer, S., Kappler, A., Haderlein, S.B., Schmidt, C., Byrne, J.M., Kleindienst, S., Vogt, C., Richnow, H.H., Obst, M., Angenent, L.T., Bryce, C., McCammon, C., Planer-Friedrich, B., 2021. A biogeochemical–hydrological framework for the role of redox-active compounds in aquatic systems. Nat. Geosci. 14, 264–272.
Ren, Y., Zhang, L., Yang, K., Li, Z., Yin, R., Tan, B., Wang, L., Liu, Y., Li, H., You, C., Liu, S., Xu, Z., Kardol, P., 2020. Short-term effects of snow cover manipulation on soil bacterial diversity and community composition. Sci. Total Environ. 741, 140454.
Routson, C.C., McKay, N.P., Kaufman, D.S., Erb, M.P., Goosse, H., Shuman, B.N., Rodysill, J.R., Ault, T., 2019. Mid-latitude net precipitation decreased with Arctic warming during the Holocene. Nature 568, 83–87.
Ruiz-Gil, T., Acuña, J.J., Fujiyoshi, S., Tanaka, D., Noda, J., Maruyama, F., Jorquera, M. A., 2020. Airborne bacterial communities of outdoor environments and their associated influencing factors. Environ. Int. 145, 106156.
Sadigh, A., Fataei, E., Arzanloo, M., Imani, A.A., 2021. Bacteria bioaerosol in the indoor air of educational microenvironments: measuring exposures and assessing health effects. Journal of Environmental Health Science and Engineering 19, 1635–1642.
Schiermeier, Q., 2008. 'Rain-making' bacteria found around the world. Nature. https://doi.org/10.1038/news.2008.632.
Schramm, P.J., Brown, C.L., Saha, S., Conlon, K.C., Manangan, A.P., Bell, J.E., Hess, J.J., 2021. A systematic review of the effects of temperature and precipitation on pollen concentrations and season timing, and implications for human health. Int. J. Biometeorol. 65, 1615–1628.
Shannon, C.E., 1948a. A mathematical theory of communication. Bell Syst. Tech. J. 27, 623–656.
Shannon, C.E., 1948b. A mathematical theory of communication. Bell System Technical Journal 27, 379–423.
Shen, F., Hegglin, M.I., Luo, Y., Yuan, Y., Wang, B., Flemming, J., Wang, J., Zhang, Y., Chen, M., Yang, Q., Ge, X., 2022. Disentangling drivers of air pollutant and health risk changes during the COVID-19 lockdown in China. npj Climate and Atmospheric Science 5, 54.
Shu, W.-S., Huang, L.-N., 2022. Microbial diversity in extreme environments. Nat. Rev. Microbiol. 20, 219–235.
Smirnova, M., Miamin, U., Kohler, A., Valentovich, L., Akhremchuk, A., Sidarenka, A., Dolgikh, A., Shapaval, V., 2021. Isolation and characterization of fast-growing green snow bacteria from coastal East Antarctica. MicrobiologyOpen 10, e1152.
Šťovíček, A., Azatyan, A., Soares, M.I.M., Gillor, O., 2017. The impact of hydration and temperature on bacterial diversity in arid soil mesocosms. Front. Microbiol. 8.
Tianjin Municipal Statistics Bureau, China (TMSBC), 2022. The Statistical Bulletin of the National Economic and Social Development of Tianjin Municipality. China.
Uk Lee, B., Lee, G., Joon Heo, K., 2016. Concentration of culturable bioaerosols during winter. J. Aerosol Sci. 94, 1–8.
van Leuken, J.P.G., Swart, A.N., Droogers, P., van Pul, A., Heederik, D., Havelaar, A.H., 2016. Climate change effects on airborne pathogenic bioaerosol concentrations: a scenario analysis. Aerobiologia 32, 607–617.
Wang, H., Ceylan Koydemir, H., Qiu, Y., Bai, B., Zhang, Y., Jin, Y., Tok, S., Yilmaz, E.C., Gumustekin, E., Rivenson, Y., Ozcan, A., 2020. Early detection and classification of live bacteria using time-lapse coherent imaging and deep learning. Light Sci. Appl. 9, 118.
Wang, Y., Zhang, S., Hong, Q., Song, H., Yang, L., Yang, K., Xu, H., Yu, F., 2022. Characteristics, non-carcinogenic risk assessment and prediction by HYSPLIT of bioaerosol released from Hospital and Municipal Sewage, China. Ecotoxicol. Environ. Saf. 246, 114131.
Wei, M., Liu, H., Chen, J., Xu, C., Li, J., Xu, P., Sun, Z., 2020. Effects of aerosol pollution on PM2.5-associated bacteria in typical inland and coastal cities of northern China during the winter heating season. Environ. Pollut. 262, 114188.
Woo, C., Yamamoto, N., 2020. Falling bacterial communities from the atmosphere. Environmental Microbiome 15, 22.
Xin, X.-F., Kvitko, B., He, S.Y., 2018. Pseudomonas syringae: what it takes to be a pathogen. Nat. Rev. Microbiol. 16, 316–328.
Xu, P., Zhang, C., Mou, X., Wang, X.C., 2020. Bioaerosol in a typical municipal wastewater treatment plant: concentration, size distribution, and health risk assessment. Water Sci. Technol. 82, 1547–1559.
Ye, L., Huang, M., Zhong, B., Wang, X., Tu, Q., Sun, H., Wang, C., Wu, L., Chang, M., 2018. Wet and dry deposition fluxes of heavy metals in Pearl River Delta Region (China): characteristics, ecological risk assessment, and source apportionment. J. Environ. Sci. 70, 106–123.
Yu, S., Zhou, X., Hu, P., Chen, H., Shen, F., Yu, C., Meng, H., Zhang, Y., Wu, Y., 2022. Inhalable particle-bound marine biotoxins in a coastal atmosphere: concentration levels, influencing factors and health risks. J. Hazard Mater. 434, 128925.
Zeng, Q., An, S., 2021. Identifying the biogeographic patterns of rare and abundant bacterial communities using different primer sets on the loess plateau. Microorganisms 9, 139.
Zhang, J., Zhou, X., Jiang, S., Tu, L., Liu, X., 2020a. Monsoon precipitation, economy and wars in ancient China. Front. Earth Sci. 8.
Zhang, S., Sun, L., Wang, Y., Fan, K., Xu, Q., Li, Y., Ma, Q., Wang, J., Ren, W., Ding, Z., 2020b. Cow manure application effectively regulates the soil bacterial community in tea plantation. BMC Microbiol. 20, 190.
Zhang, T., Chen, Y., Cai, Y., Yu, Y., Liu, J., Shen, X., Li, G., An, T., 2023. Abundance and cultivable bioaerosol transport from a municipal solid waste landfill area and its risks. Environ. Pollut. 320, 121038.
Ziemba, L.D., Beyersdorf, A.J., Chen, G., Corr, C.A., Crumeyrolle, S.N., Diskin, G., Hudgins, C., Martin, R., Mikoviny, T., Moore, R., Shook, M., Thornhill, K.L., Winstead, E.L., Wisthaler, A., Anderson, B.E., 2016. Airborne observations of bioaerosol over the southeast United States using a wideband integrated bioaerosol sensor. J. Geophys. Res. Atmos. 121, 8506–8524.
Zimmerman, A.E., Howard-Varona, C., Needham, D.M., John, S.G., Worden, A.Z., Sullivan, M.B., Waldbauer, J.R., Coleman, M.L., 2020. Metabolic and biogeochemical consequences of viral infection in aquatic ecosystems. Nat. Rev. Microbiol. 18, 21–34.